

Coplanar-PGL Transitions on High Resistivity Silicon Substrate in the 57–64 GHz Band and Influence of the Probe Station on the Performances

Marjorie Grzeskowiak^{1, *}, Julien Emond¹, Gaelle Lissorgues², Stephane Protat¹, Frederique Deshours³, Elodie Richalot¹, and Odile Picon¹

Abstract—We present Coplanar-Planar Goubau Line (PGL) transitions designed on high-resistivity Silicon to characterize a PGL using microwave probing. These transitions are optimized in the 57–64 GHz frequency band to present excellent electrical performances despite the field disturbance of the measurement setup. As the transitions are positioned on a probe station chuck, a glass substrate is added between the transition under test and the metallic chuck to minimize the disturbance. 3-D full-wave electromagnetic field simulations performed on a commercial software and on-wafer measurements show almost comparable results in term of scattering matrix parameters. Low losses are attained with a measured average transmission parameter of 2.5 dB at 60 GHz for a length of 8 mm of a back-to-back structure with the transitions at the extremities. The measured average insertion loss and return loss per transition are better than 1.36 dB and 11 dB, respectively, with a bandwidth greater than 7% at 60 GHz for a length of 1 mm (about a half of the wavelength at 60 GHz).

1. INTRODUCTION

The 57 to 64 GHz frequencies band is particularly attractive because of the licence-free accessible for Ultra-Wide Band (UWB) signals, the miniaturization of the systems and the security aspect of short range communications due to high atmospheric losses at 60 GHz [1]. In the 57–64 GHz band, the on-wafer characterization of transmission lines or any microwave devices, with a probe station, requires generally a coplanar access; the most usual configuration is the Ground-Signal-Ground (GSG) one.

Several millimeterwave transitions have been studied, dedicated to the device characterization, the interconnection between different transmission lines or circuit layers together. A lot of them are 3D transitions including via holes [2–6]. Transitions without any via hole [7–9] present the advantage of an easier fabrication process. A microstrip-to microstrip vertical via-less multilayer transition [7], based on a broad-side coupler structure, exhibits less than 0.7 dB of loss in the band from 57 to 66 GHz. A uniplanar Finite Ground Coplanar Waveguide (FGCPW) to microstrip line transition [8] provides a 0.2 dB insertion loss at 94 GHz and a return loss better than -17 dB from 85 GHz to 100 GHz and could be useful for CPW-probe to microstrip circuit measurements. A coaxial-to-strip line transition shows a return loss better than 10 dB and an insertion loss better than 6 dB up to 67 GHz for a back-to-back structure of 1.55 mm length [9]. A transition, from coplanar waveguide to dielectric waveguide, is investigated for the integration of active devices in dielectric waveguides, and allows a maximum insertion loss of 1.7 dB and return loss better than 15 dB over 7% bandwidth at 60 GHz for a total length of 7 mm [10]. Grounded Coplanar Waveguide-Microstrip (GCPW-MS) transition on 8 μm -thick BCB deposited on a metalized low resistivity wafers for a 1 cm back-to-back structure can facilitate the

Received 7 November 2013

* Corresponding author: Marjorie Grzeskowiak (marjorie.grzeskowiak@univ-mlv.fr).

¹ Université Paris-Est, ESYCOM (EA 2552), UPEMLV, ESIEE-Paris, CNAM, Marne-la-Vallée F-77454, France. ² Université Paris-Est, ESYCOM, UPEMLV, ESIEE-Paris, CNAM, Cité Descartes, BP99, Noisy le Grand 93162, France. ³ UPMC université Paris 06, L2E, 4 place Jussieu, 75252 Paris Cedex 05, France.

characterization of components driven by MS transmission lines up to 77 GHz with insertion loss better than 2 dB [11].

A few transitions have been designed in order to excite the Goubau mode. The PGL lines have already been characterized for higher frequencies by means of transitions: PGL to $50\ \Omega$ microstrip line circuit transitions on ceramic substrate (0.254 mm alumina), dedicated to feed PGL loads and power divider/combiner, present, for a 16 mm total length of the back-to-back structure, a 4 dB transmission parameter from 40 GHz to 60 GHz [12], or dedicated to feed couplers with short range (60 GHz) radio [13], a coplanar-Goubau Line transition on Duroid 5880 provides a 5–10 dB insertion loss and a return loss better than -12 dB from 140 GHz to 220 GHz for a back-to-back structure [14] and recently a “smooth” transition to match a periodic leaky-wave antenna at millimeter wave frequencies with PGL impedance to a coplanar waveguide [15]. The results for the transitions to excite the PGL mode [12–15] seem less efficiency than for the other ones [2–11]: the PGL doesn’t need a ground plane, contrary to the coplanar or micro-strip modes and the conversion from coplanar or micro-strip modes to PGL mode generates other modes or losses.

We have recently developed a low loss PGL structure on high resistivity silicon with a measured average attenuation of 0.064 dB/mm on the whole 57–64 GHz band [16]. The low losses and the low dispersion of the PGL, combined with a simple fabrication process, make it a good candidate for UWB applications. This line, because of its possible integrated circuit fabrication processes [12–15], can be used to realize functions without the necessity to report a ground plane: the width of the strip, the thickness and the relative permittivity of the substrate can be selected to favor the confinement of the field to reduce the attenuation or, in inverse, to favor the radiation of the PGL to couple the lines together (the lines must be curved to optimize the coupling) and realized couplers for instance [14]. It has been compared recently with a Inverted Microstrip Line (IML), that offers a natural mechanical encapsulation, protecting the device from any electromagnetic radiation [17] with the same characteristics of propagation mode, but with a more complex technological process: the PGL can be replaced by IML to offer a ground plane, or to prevent from the sensibility to the electromagnetic radiation. The characterization of PGL structures requires coplanar waveguide probe pads. In order to perform on-wafer measurement, transitions from the excitation access to the PGL line must be optimized. This paper presents coplanar to PGL transitions on high-resistivity Silicon. In Section 2, we describe the PGL structure and notice the variation of the different PGL losses because of the addition of the transitions. To take into account the measurement setup and avoid its disturbance, a glass substrate is added and we simulate the electric field distribution and the losses for different configurations. In Section 3, we report the evolution of the reflection and transmission parameters versus the measurement setup. In Section 4, we conclude this work.

2. DESCRIPTION OF THE COPLANAR-TAPERED PGL TRANSITION

Figure 1 illustrates the studied transitions. The transition is actually operating as an impedance and field matching transformer between coplanar probes and PGL and has been designed to measure electrical characteristics of the PGL. The PGL can be compared to a high frequency band line, so in order to decrease the cut-off frequency of the PGL; we have to increase the substrate thickness and the relative permittivity [16].

The coplanar to PGL transition have been realized on a high resistivity silicon substrate ($60\ \Omega\cdot\text{m}$)

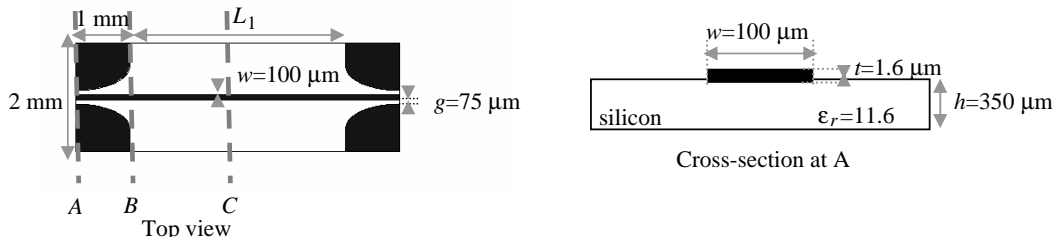


Figure 1. Top view of the coplanar to PGL transition and cross-section of the PGL.

of 350 μm height. The back-to-back structures, constituted of both similar transitions of 1 mm length and different lengths of PGL (L_1 can be equal to the values 2; 4; 6; 8; 10 and 20 mm), are designed with a strip width of 100 μm and a gold metallization thickness of 1.6 μm (Figure 1).

The characteristic impedances are equal respectively to 50 Ω and 75 Ω for the coplanar access and the PGL. However, the PGL proposes a large variety of impedances to interconnect the components: characteristic impedances from 35 to 93 Ω are obtained in the 57–64 GHz frequency band for a line width between 50 μm and 500 μm .

The elliptical shape of the transition allows a continuous increase of the coplanar line impedance with the increase of the slot widths. The maximal slot widths, at the end of the transition, are chosen so that the characteristic impedance of the CPW is equal to the one of the GPL (75 Ω).

The length of the back-to-back structure is equal to 8 mm: this value seems to be chosen arbitrarily but it corresponds to the best performance for the transition with the measurement setup. It is reported in 3 paragraphs. A 8 mm PGL is compared with a 8 mm back-to-back structure, constituted of both similar transitions of 1 mm length and a 6 mm PGL (L_1 is equal to 6 mm in the Figure 1). A deembedding to precisely characterize the transitions will be done in the 3.2 paragraph.

3. 3-D ELECTROMAGNETIC SIMULATIONS

3.1. S -parameters of the Coplanar-PGL Transitions

The geometry of the coplanar-PGL transition has been optimized using ANSYS HFSS (High Frequency Structural Simulator) software in order to reduce mismatching losses and field matching transformation between coplanar probes and PGL. The strip width (W) remains unchanged along the transition and the slots (g) at the coplanar input access are designed to obtain an impedance of 50 Ω .

The scattering parameters of the back-to-back structure with and without the transitions are reported in Figure 2 and are calculated versus the characteristic impedance of the propagation line in contact with the simulation wave-port: the PGL and the coplanar line present respectively a

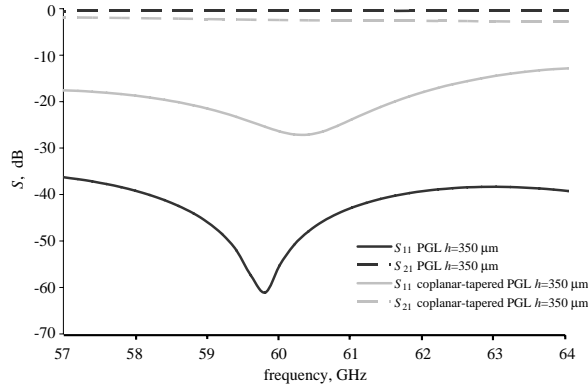


Figure 2. Simulated insertion loss and return loss of back-to-back structures with and without the coplanar-tapered PGL transition in 57–64 GHz frequency band for a total length of 8 mm on 350 μm silicon substrate.

Table 1. Simulated insertion loss, return loss and energy conservation at 60 GHz of a back-to-back structure of 8 mm length with and without the coplanar-tapered PGL transitions in 57–64 GHz frequency band.

at 60 GHz	PGL of 8 mm length	Transitions + PGL of 6 mm length
S_{11}	0.013	0.049
S_{21}	0.958	0.900
Energy conservation (%)	91.8	81.2

characteristic impedance of $75\ \Omega$ and $50\ \Omega$. This comparison is just dedicated to verify the impedance matching of the transition versus the reflected and transmitted powers.

In order to evaluate the influence of the transitions on the PGL losses, we report on Table 1 the values of S_{11} and S_{21} parameters at 60 GHz and we evaluate the energy conservation corresponding of the $(s_{11}^2 + s_{21}^2)$ term.

The energy conservation is equal to 91.8% for the PGL and it is reduced to 81.2% for the PGL excited at the extremities by the transitions. The difference could be due to the excitation by the coplanar line to other modes and to the radiation or dielectric losses. To reduce the simulation time, a symmetric plane is used in the middle of the PGL, and we can verify the propagation of one mode at the beginning of the transition, the coplanar mode. The slot mode isn't observed because of the symmetry of the structure. Nevertheless, with the PGL structures without the transitions, several modes can propagate on the PGL.

3.2. Losses and Field Distribution with the Measurement Setup

During the measurement, the back-to-back structures will be placed on the chuck of a Microtech probe station and each port will be connected to ground-signal-ground probes [18]. The GSG configuration of the probes supports a coplanar waveguide mode, but, when the probes approach the metalized chuck beneath the wafer, other modes appear, as the MS between the probe conductor and the metalized chuck [19]. The effect of the metalized chuck, that modified the performances of the device under test, can be minimized by placing low-permittivity foam between the structure and the metalized chuck [20]. However, the effect of the metalized chuck cannot be totally removed, because of the limited space between the probes and the chuck.

In this study, a glass substrate of $500\ \mu\text{m}$ thickness is added underneath the silicon to avoid the disturbance of the back-to-back structure by the proximity of the metalized chuck. So to take into account the measurement setup, the same glass substrate is added in HFSS simulations, as shown on Figure 3. The chuck is modeled by a boundary finite conductivity ($\sigma = 1.1 \cdot 10^6\ \text{S}\cdot\text{m}^{-1}$ for the steel stainless) below the glass substrate.

The simulated electric field distribution along the transition is depicted on Figure 4 at different planes. For the propagation mode of the PGL, the field must be confined around the strip and decay in the transverse plane. We can see that the effect of the metalized chuck on the field is attenuated by the addition of the glass substrate in the *B* and *C* planes, while it isn't negligible in the *A* plane: the coplanar mode is clearly disrupted by the metalized chuck.

In a first step, the energy conservation is evaluated and compared versus different substrate configurations for the back-to-back structures of 8 mm length with and without the transitions at 60 GHz. The scattering parameters and the energy conservation are reported in Table 2. The energy conservation that is equal to 91.2% for the 8 mm length PGL line without the transitions is reduced to 80.9% with the transitions, and breaks down to 70.5% in presence of the chuck and with the transitions. The difference could be due essentially to the excitation by the coplanar line to other modes [16] or to the confinement of the field along the edge of the tapered transition (Figure 5). Nevertheless, the metalized chuck, that decreases the energy conservation of the PGL with the transitions down to 55.3%

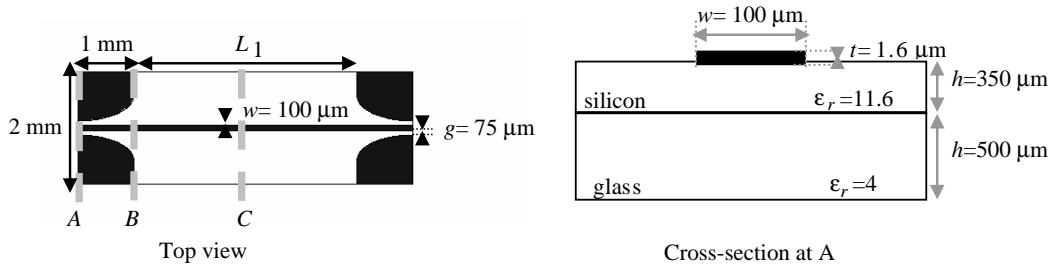


Figure 3. Top view of the coplanar to PGL transition and cross-section of the PGL with the measurement setup.

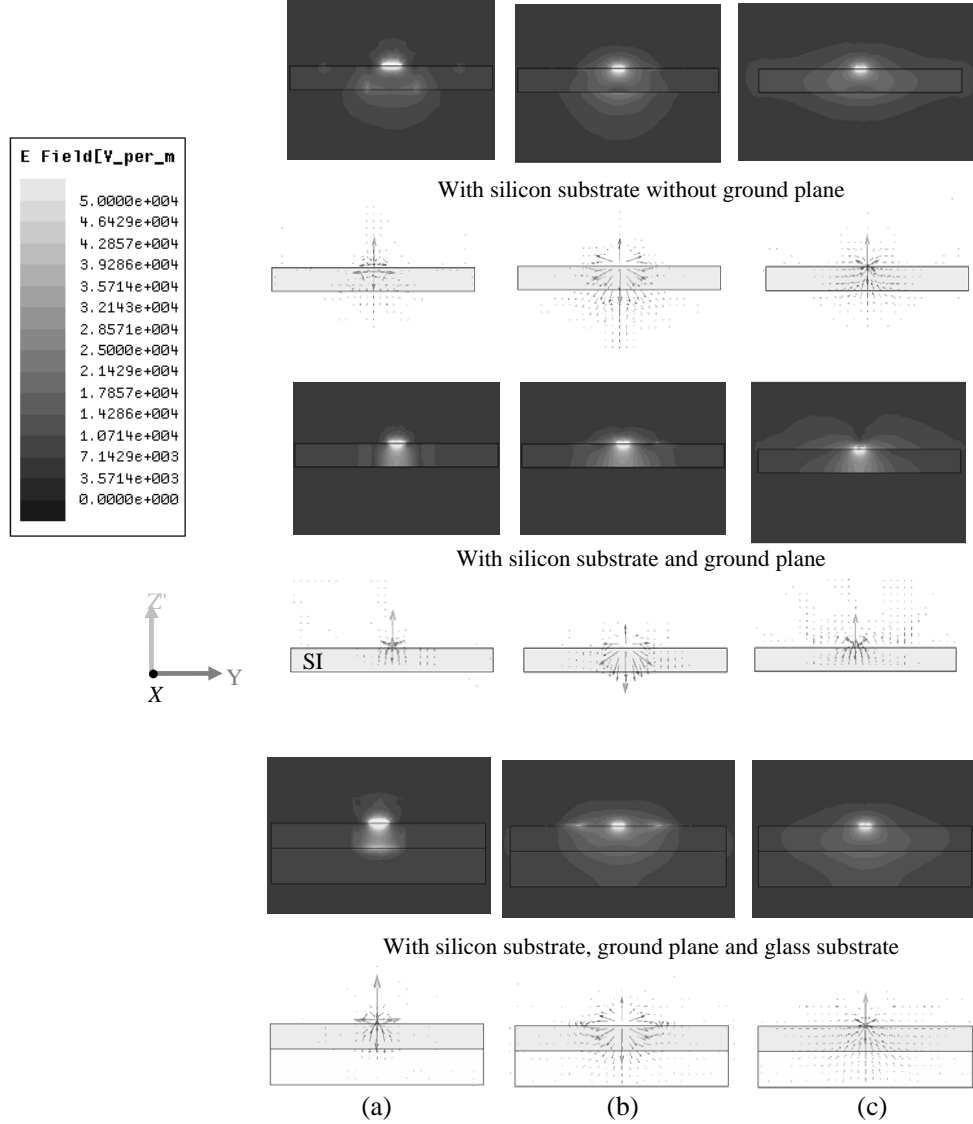


Figure 4. Simulated cross-section E -field distributions along the coplanar-tapered PGL transition, (a) plane A, (b) plane B, (c) plane C of the Figure 3.

for a $350\ \mu\text{m}$ thick of silicon, can be minimized by placing glass substrate between the silicon substrate and the metalized chuck: then, the energy conservation is equal to 70.5%.

In a second step, the losses of the PGL are calculated and compared with and without the transitions without the chuck (Table 3): in the Table 2, it has been verified that the chuck didn't modify the total energy conservation of the PGL: the energy conservation stays around 93%. It can be explained by the field confinement around the strip not modified by the metalized plane. The characteristics of the first propagation mode are the same ones for the PGL structure with and without ground plane. In order to qualify and quantify the losses, we simulate the PGL line in free-space, or in a metallic waveguide, with perfect lossless dielectric or with a PEC (Perfect Electrically Conductor). The simulation in a metallic waveguide allows cancelling the losses by radiation, and the substitution of a PEC and of lossless silicon instead of gold and silicon leads, respectively, to deduct the metallic losses and the dielectric losses.

The transition addition allows finding almost the same values of loss by de-embedding for the PGL. Nether less, we have a slightly difference with the transition: the radiation losses are increased. We would like to calculate the radiation of the transition.

We inserted the structure, constituted of $350\ \mu\text{m}$ of silicon on $500\ \mu\text{m}$ of glass with and without the

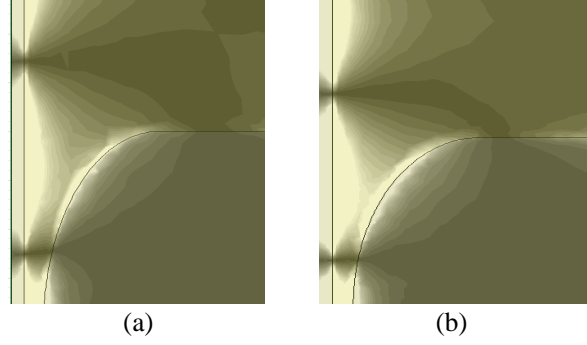


Figure 5. Simulated E-field magnitude on the top of the PGL structure (with the scale of the Figure 4). (a) Without the chuck. (b) With the chuck.

Table 2. Simulated S -parameters and energy conservation at 60 GHz for the back-to-back PGL structures of 8 mm with or without the coplanar-tapered PGL transitions in presence or in absence of the chuck.

Structure		S_{11}	S_{21}	$S_{11}^2 + S_{21}^2$ %
PGL of 8 mm	350 μm of Silicon	0.013	0.958	91.8
PGL of 8 mm	350 μm of Silicon + chuck	0.011	0.963	93.1
PGL of 8 mm	350 μm of silicon +500 μm of Glass	0.020	0.955	91.2
PGL of 8 mm	350 μm of silicon +500 μm of Glass + chuck	0.006	0.962	92.5
PGL of 6 mm + 2 transitions	350 μm of Silicon	0.049	0.900	81.2
PGL of 6 mm + 2 transitions	350 μm of Silicon + chuck	0.053	0.742	55.3
PGL of 6 mm + 2 transitions	350 μm of silicon +500 μm of Glass	0.037	0.899	80.9
PGL of 6 mm + 2 transitions	350 μm of silicon +500 μm of Glass + chuck	0.012	0.840	70.5

Table 3. Simulated qualification and quantification of different losses (dB/mm) of the PGL at 60 GHz of the back to-back structure of 4 mm length in considering the influence of the transitions without the chuck.

at 60 GHz	PGL	Transition+PGL
All losses α	0.057	0.061
Dielectric losses α_d	0.009	0.09
Metallic losses α_c	0.032	0.32
Radiation losses α_r	0.016	0.02

Table 4. Simulated reflection parameter, transmission parameter and energy conservation versus the structure in free space or in PEC waveguide for a 8 mm length back-to-back structure.

structure	in	S_{11}	S_{21}	$S_{11}^2 + S_{21}^2$ (%)
PGL	Free space	0.020	0.955	91.2
	PEC waveguide	0.001	0.962	92.5
PGL + chuck	Free space	0.006	0.962	92.5
	PEC waveguide	0.012	0.979	95.8
PGL + transitions	Free space	0.037	0.899	80.9
	PEC waveguide	0.042	0.932	87.0
PGL + transitions + chuck	Free space	0.012	0.840	70.5
	PEC waveguide	0.019	0.867	75.2

transitions in a metallic waveguide and we compare with the same structure in free-space (Table 4).

Without the transitions, for the structure in a metallic waveguide, the energy conservation is equal to 92.5% and comparable with the 91.2% for the structure in free space. With the transitions, for the structure in a metallic waveguide, the energy conservation is equal to 87% in comparison with the 80.9% of the structure in free space: the PGL associated with the transitions has 6.1% radiated losses. So, the both transitions increase the radiation of the global structure.

4. THE TRANSITION DESIGN AND MEASUREMENT

The back-to-back structures have been achieved using standard photolithography techniques for two different widths of strip: $w = 50 \mu\text{m}$ and $w = 100 \mu\text{m}$.

We present the results of the back-to-back structures for the $100 \mu\text{m}$ strip and the de-embedded results are compared for the both transitions ($w = 50 \mu\text{m}$ and $100 \mu\text{m}$).

The scattering parameters of the back-to-back structures are measured with a Vectorial Network Analyzer (VNA) and compared with the simulated ones, for a $100 \mu\text{m}$ strip. A Line Reflect Match (LRM) calibration was performed using a kit to eliminate parasitic errors that may affect the measurement results, like the probing effect and the measurement setup [18].

We reported in Figures 6 and 7, the scattering parameters of the back-to-back structure with and without the chuck, with and without the coplanar-tapered PGL transition in the 57–64 GHz frequency band for a total length of 8 mm and for a strip width of $100 \mu\text{m}$. ($L_1 = 6 \text{ mm}$ correspond to the best obtained results, due to correct matching).

PGL0 is printed on a $350 \mu\text{m}$ thick silicon substrate over $500 \mu\text{m}$ glass without the coplanar-tapered transition and simulated in free space, PGL1 contains the coplanar-tapered PGL transition and is printed on a $350 \mu\text{m}$ thick silicon substrate over $500 \mu\text{m}$ glass on metalized chuck and PGL2 is PGL1 simulated without the metalized chuck.

The effect of the metalized chuck cannot be totally removed and the transition, even with the addition of glass substrate, is disturbed by the measurement setup:

- The matching of the back-to back structure, less than 40 dB for the studied frequency band for a PGL without the transitions and without the metalized chuck, is less than 15 dB for a PGL with the transition and with the metalized chuck.
- The insertion loss pass from 0.4 dB without transition and metalized chuck to 1.7 dB at 60 GHz in considering the transition and the chuck in simulation and a maximum of 4 dB is obtained in measurement.
- At 60 GHz the measured energy conservation of 59.5% is less than the simulated calculated one of 70.5% ($L_1 = 6 \text{ mm}$).

We focus on a PGL of $50 \mu\text{m}$ and $100 \mu\text{m}$ wide strips, which present respectively 92Ω and 73Ω characteristic impedances. The S -parameters of the both transitions between the coplanar measurement

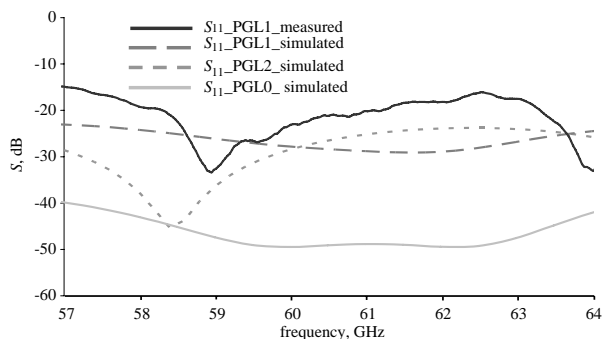


Figure 6. Simulated and measured return loss (strip of $100 \mu\text{m}$ and slots of $75 \mu\text{m}$ for the coplanar line).

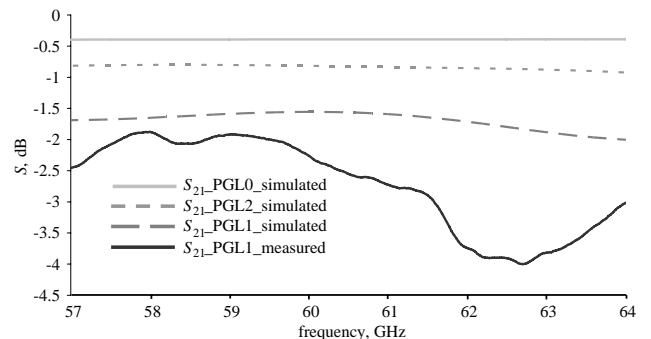


Figure 7. Simulated and measured insertion loss of (strip of $100 \mu\text{m}$ and slots of $75 \mu\text{m}$ for the coplanar line).

access and a PGL of width $w = 50$ or $100 \mu\text{m}$, have been de-embedded from measurements and reported on Figures 8 and 9.

The transition for $w = 100 \mu\text{m}$ presents better performances than this one for $w = 50 \mu\text{m}$: the measured return loss of the transition is lower than -10 dB on the 57–64 GHz frequency band (Figure 8) and the insertion loss is equal to 1.36 dB (Figure 9) at 64 GHz for a strip width of $100 \mu\text{m}$. The difference between simulation and measurement for the return loss and the transmission ones may be caused by mechanical misalignments between the reference planes for the exciting mode due to the position of the probes: in measurement the probes aren't just positioned at the beginning of the transition. This phenomenon could be attenuated by the addition of a length of constant coplanar line in order to position the probes. Nevertheless, the de-embedded insertion loss per transition is approximately 1.36 dB from 57 to 64 GHz; this low-loss transition allows accurate measurement of PGL attenuation and phase constant: the measured loss for the PGL with $w = 100 \mu\text{m}$ is 0.064 dB/mm [16].

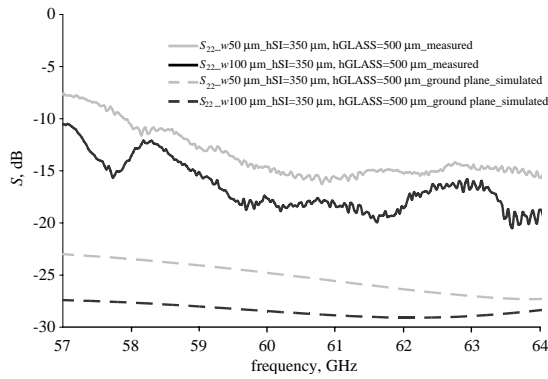


Figure 8. Simulated and measured return loss per transition (strip-line width of $50 \mu\text{m}$ and $100 \mu\text{m}$).

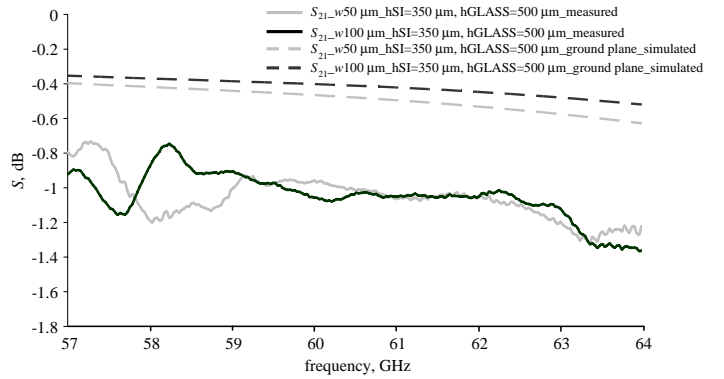


Figure 9. Simulated and measured transmission losses per transition (strip-line width of $50 \mu\text{m}$ and $100 \mu\text{m}$).

5. CONCLUSION

In this paper, coplanar-tapered PGL transitions were successfully designed, fabricated and characterized from 57 to 64 GHz. The low loss attenuation obtained for the PGL on high resistivity Silicon explains the necessity to realize low loss transition for such structures. The back-to-back structures are characterized on a probe station and disrupted by the metalized chuck. In order to attenuate all signals between the back-to-back structures and the metalized chuck, a glass substrate is added inside the transition-under-test and the metallic probe station chuck. The measurement setup is taken into account in FEM simulation and comparable results in term of reflection and transmission parameters are obtained. The design of transitions is verified from the back-to-back performance with insertion loss of 2.5 dB at 60 GHz for a length of 8 mm. Performances for the transition with less than 1.36 dB insertion loss and higher than 10 dB return loss in the 57–64 GHz band were obtained by de-embedding for a PGL with $w = 100 \mu\text{m}$.

REFERENCES

1. Kuri, T., K. Kitayama, A. Stohr, and Y. Ogawa, “Fiber-optic millimeter-wave downlink system using 60 GHz-band external modulation,” *Journal of Lightwave Technology*, Vol. 17, 799–806, 1999.
2. Yang, T. H., C. F. Chen, T. Y. Huang, C. L. Wang, and R. B. Wu, “A 60 GHz LTCC transition between microstrip line and substrate integrated waveguide,” *Asia-Pacific Conference Proceedings — Microwave Conference Proceedings*, Vol. 1, 2005.
3. Bulja, S. and D. Mirshekar-Syahkal, “Novel wideband transition between coplanar waveguide and

- microstrip line,” *IEEE Transactions on Microwave Theory and Techniques*, Vol. 58, No. 7, 1851–1857, 2010.
4. Patrovsky, A., M. Daigle, and K. Wu, “Millimeter-wave wideband transition from CPW to substrate integrated waveguide on electrically thick high-permittivity substrates,” *2007 European Microwave Conference*, 138–141, 2007.
 5. Stephens, D., P. R. Young, and I. D. Robertson, “Millimeter-wave substrate integrated waveguides and filters in photoimageable thick-film technology,” *IEEE Transactions on Microwave Theory and Techniques*, Vol. 53, No. 12, 3832–3838, 2005.
 6. Boone, J., S. Krishnan, and S. Bhansali, “Silicon based vertical micro-coaxial for high frequency packaging technologies,” *Progress In Electromagnetics Research B*, Vol. 50, 1–7, 2013.
 7. Enayati, A., S. Brebels, W. Deraedt, and G. A. E. Vandenbosch, “Vertical via-less transition in MCM Technology for millimetre-wave applications,” *Electronics Letters*, Vol. 46, No. 4, 287–288, 2010.
 8. Gauthier, G. P., L. P. Katehi, and G. M. Rebeiz, “W-band finite ground coplanar waveguide (FGCPW) to microstrip transition,” *IEEE MTT-S Int. Microw. Symp. Dig.*, Vol. 1, 107–109, 1998.
 9. Xia, L. and R. Xu, “Broadband LTCC transition from coaxial connector to stripline for 60 GHz application,” *International Conference on Computational Problem-Solving (ICCP)*, 52–54, 2012.
 10. Zandieh, A., N. Ranjkesh, S. Safavi-Naeini, and M. Basha, “A low loss CPW to dielectric waveguide transition for millimeter-wave hybrid integration,” *Antennas and Propagation Society International Symposium (APSURSI)*, 1–2, 2012.
 11. El-Gibari, M., D. Averty, C. Lupi, M. Brunet, H. Li, and S. Toutain, “Ultra-broad bandwidth and low-loss GCPW-MS transitions on low k -substrates,” *Electronics Letters*, Vol. 46, No. 13, 931–933, 2010.
 12. Xu, Y., C. Nerguizian, and R. G. Bosisio, “Wideband planar goubau line integrated circuit components at millimetre waves,” *IET Microwave, Antennas Propagation*, Vol. 5, No. 8, 882–885, 2011.
 13. Treizebré, A. T. Akalin, and B. Bocquet, “Planar excitation of goubau transmission lines for THz BioMEMS,” *IEEE Microwave and Wireless Letters*, Vol. 15, No. 12, 886–888, 2005.
 14. Xu, Y. and R. G. Bosisio, “Wideband planar Goubau line (PGL) couplers and six-port circuits compatible with short range (60 GHz) radio,” *IET Microwaves, Antennas Propagation*, Vol. 7, No. 12, 985–990, 2013.
 15. Sanchez-Escuderos, D., M. Ferrando-Battaler, J. I. Herranz, M. Cabedo-Fabres, “Periodic leaky-wave antenna on planar Goubau line at millimeter-wave frequencies,” *IEE Antennas and Wireless Propagation Letters*, Vol. 12, 1006–1009, 2013.
 16. Emond, J., M. Grzeskowiak, G. Lissorgues, S. Protat, F. Deshours, E. Richalot, and O. Picon, “A low planar Goubau line and a coplanar-PGL transition on high resistivity Silicon substrate in the 57–64 GHz band,” *Microwave and Optical Letters*, Vol. 54, No. 1, 164–168, 2012.
 17. Grzeskowiak, M., J. Emond, S. Protat, G. Lissorgues, F. Deshours, E. Richalot, and O. Picon, “Optimization on of a quasi loss less air-cavity inverted microstrip line form microwave frequencies and comparison with the coplanar line at 60 GHz,” *Progress In Electromagnetics Research*, Vol. 43, 67–78, 2013.
 18. “On-wafer vector network analyzer calibration and measurements,” Application Note, Cascade Microtech, Beaverton, OR.
 19. Safwat, M. E., “Study of microstrip mode in RF on-wafer probes,” *Microwave and Optical Letters*, Vol. 45, No. 4, 324–328, 2005.
 20. Ghaffar, F. A. and A. Shamim, “Design of silicon-based fractal antennas,” *Microwave and Optical Letters*, Vol. 55, No. 1, 180–186, 2013.